Research Journal of Applied Sciences, Engineering and Technology 6(15): 2799-2806, 2013
DOI:10.19026/rjaset.6.3788
ISSN: 2040-7459; e-ISSN: 2040-7467

Submitted: December 31, 2012 Accepted: February 08, 2013 Published: August 20, 2013

**Research Article**

# Experimental Investigation to the Kinematics of a Blue Spotted Ray like Underwater Propulsor

Jianhui He and Yonghua Zhang
Department of Mechatronic Engineering, Taizhou Vocational and Technical College, Taizhou, 318000, China

**Abstract:** Engineers have long been impressed by the swimming speed and agility of fish. Their research effort has been focusing on the development of a new technique of propulsion by mimicking biological fish. The aim of the present work is to develop a biological inspired underwater propulsor that emulates the performance of bluspotted ray. We first measured the morphology and captured the movement of a real bluespotted ray to provide some useful references for biomimetic mechanism design. By virtue of the modular and reconfigurable design concept, a bluspotted ray like underwater propulsor was considered and developed. An experiment system was set up to investigate the effect of various kinematic parameters including frequency, amplitude, wavelength on the propulsion velocity, thrust and efficiency of the fish robot. The results show that the designed biomimetic underwater propulsor is able to propel itself effectively.

**Keywords:** Bluespotted ray, experimental investigation, kinematics, underwater propulsor

## INTRODUCTION

Fish swimming is usually classified into a variety of different modes. For example, there are about 20 locomotion modes that have been identified in steady swimming so far (Webb, 1994). This diversity comes from different combinations of undulation of flexible bodies and unsteady flapping of body-attached fins. Morphologically, fish fins fall into two categories: median fins (e.g., dorsal fins, ventral fins and caudal fins) and paired fins (e.g., pectoral fins and pelvic fins). Paired fins are employed mostly in motion stabilization, maneuvering and braking (Webb, 1973; Blake, 1979; Vogel, 1994; Standen, 2008). Indeed, in many species (e.g., rajiform), pectoral fins are often the primary locomotion devices (Videler, 1993). Swimming performance shows that pectoral propulsors in some species are capable of generating thrusts that can power speeds up to 10 body lengths per second (Walker and Westneat, 2002). In addition, these species are highly maneuverable in complex three-dimensional reef habitats.

Bio-inspired robotics is one of the areas of interest in underwater vehicle research in recent years (Chong *et al*., 2009; Wernli, 1999; Lionel, 2006). By virtue of robotics technology, engineers hope to achieve highly efficient propulsion of fish robots. Hence, this had led to the research and development of robotic fish of different types Kato, 2000; Saimek and Li, 2004; MacIver *et al*., 2004; Leonard, 1995; Low and Willy, 2006). Pectoral fin based swimming is commonly referred to as the rajiform mode by Breder (1926). In addition to being agile, prior research has also suggested that they are highly efficient for movement at low velocities (Blake, 1983; Lighthill and Blake, 1990).

Two goals motivate the current study. First, we want to make clear the regularities that the rajiform fish such as bluespotted ray possesses to control their motion. Second, biomimetic bluespotted ray like underwater propulsor may provide an outstanding superior in applications such as environmental monitoring and military scouting than traditional screw propeller (MacIver *et al*., 2004; Epstein *et al*., 2006). Thus, the objective of the current study is to measure the morphology of a real bluespotted ray (*Taeniura lymma*) and to obtain the kinematic parameters during cruising, turning, take-off and landing motion. Based on these, we later developed a bio-robotic bluespotted ray and investigated the effect of undulating frequency, amplitude, wavelength on its propulsion velocity, thrust and efficiency respectively.

## BIOLOGICAL INSPIRATION

**Morphology:** The mechanism design was initiated by understanding the physical characteristics of *Taeniura lymma*. Biological research on *Taeniura lymma*, such as morphology and kinematics, provides many valuable data.

**Corresponding Author:** Jianhui He, Department of Mechatronic Engineering, Taizhou Vocational and Technical College, Taizhou, 318000, China

Fig. 1: Taeniura lymma

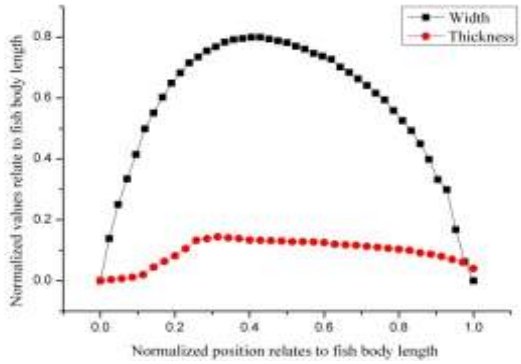


Fig. 2: External morphology measurments of our observed biomimetic object (the body length of *Taeniura lymma* is 16.3 cm)

**External morphology:** The bluespotted ray (*Taeniura lymma*) is a species of stingray in the family Dasyatidae. Found from the intertidal zone to a depth of 30 m, this species is common throughout the tropical Indian and western Pacific Oceans in nearshore, coral reef-associated habitats. It is a fairly small ray, not exceeding 35 cm in width, with a mostly smooth, a laterally compressed body, oval pectoral fin disc, large protruding eyes, and a relatively short and thick tail with a deep fin fold underneath (Fig. 1). It can be easily identified by its striking color pattern of many electric blue spots on a yellowish background, with a pair of blue stripes on the tail (Compagno, 2005).

Figure 2 illustrates the external morphology of our present observed biomimetic object. The normalized values associated with the organism include width and thickness of the body, labeled by –■– and –●– in Fig. 2 respectively. Our early study on Carangiform fish revealed that: the absolute sizes in appearance between individuals may be different, but no obvious differences were observed when converted these sizes to be dimensionless with using the total body length, indicating that dispite individual differences, the distribution proportions of fish may be similar (Zhang *et al*., 2007). The actual geometry of Taeniura Lymma was later replicated by processing profile images from videos of the actual animal.

**Internal anatomical structure of its widely expanded pectoral fin:** As to the internal anatomical structure of *Taeniura Lymma's* pectoral fin, Rosenberger had done many meanful works (Rosenberger *et al*., 1999; Rosenberger, 2001).

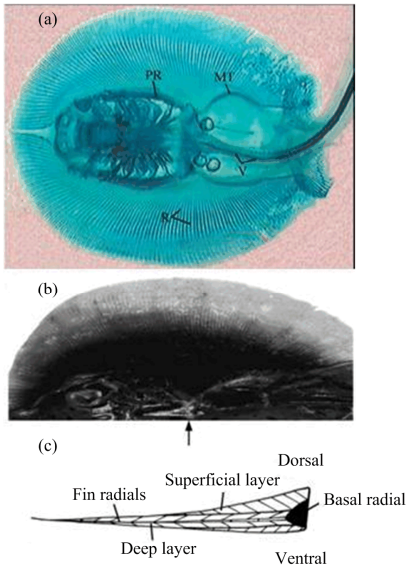


Fig. 3: Dissection of the musculature and an X-ray of *Taeniura lymma*. (a) Dorsal view of a cleared and stained skeleton of Potamotrygon motoro, a species closely related to *Taeniura lymma*. MT, metapterygium; PR, propterygium; R, radials; V, vertebrae. (b) Dorsal view dissection of pectoral abductor muscles in *Taeniura lymma*. (c) Schematic drawing of a pectoral fin cross section (at arrow) showing superficial and deep muscles, fin radials and the basal radial (photos are adopted and modified from Rosenberger *et al*. (1999))

Figure 3 shows a gross dissection of the musculature and an X-ray of *Taeniura lymma* to determine the structure of the different layers of muscle and skeleton in the pectoral fins. In *Taeniura lymma*, the fin radials extend out from the basal radials to the fin margin and are segmented along their length. The radials are longest in the middle portion of the fin and become progressively shorter moving anteriorly and posteriorly (Fig. 3a). Dissections of the pectoral fin musculature of *Taeniura lymma* reveal the working principle of muscle. In general, the dorsal (abductor) muscle are used to elevate the fin and the ventral (adductor) muscle are used to depress the fin. They are composed of superficial and deep layers (Fig. 3c), each surrounded by tendinous sheaths (Fig. 3b and c). The superficial layer consists mainly of red muscle, which is used for the pectoral fins lasting periodic motion. Deep layer consists mainly of white muscle, often used for the transient motion (Calvert, 1983). By alternately lengthening or shortening dorsal muscle and ventral muscle, *Taeniura lymma* is able to oscillate the fin ray, thus produce a traveling wave downwards pectoral fin surface. Rosenberger proposed that *Taeniura lymma* increases speed and fin-beat frequency by changing onset times in all the muscles along the fin instead of changing the duration of muscle activity to increase swimming velocity (Rosenberger *et al*., 1999).

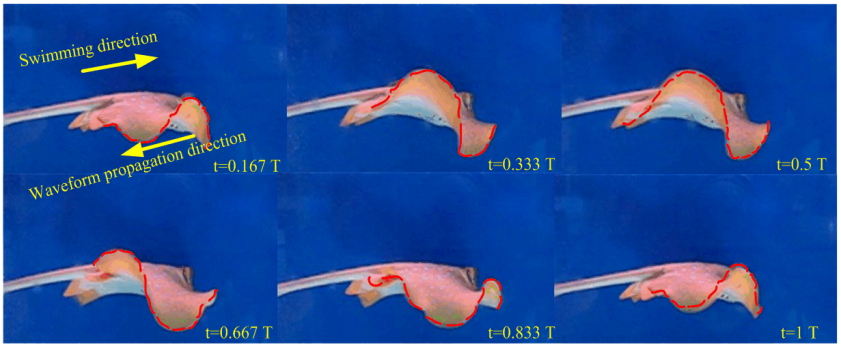


Fig. 4: Successive lateral video images of *Taeniura lymma* during steady forward swimming in a tank

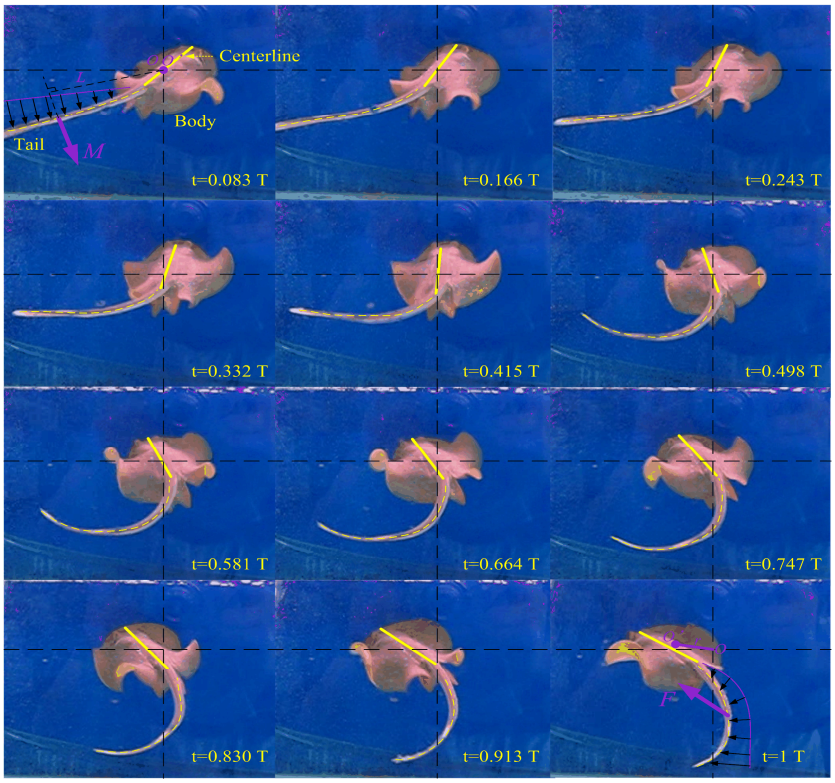


Fig. 5: An anticlockwise 90° turning of *Taeniura lymma* T: Turning cycle; M: Rotating torque; F: Force; V: Velocity; O: Center of gravity

**Kinematics:** The swimming mode of bluespotted ray is called rajiform swimming. In rajiform mode, found in stingrays and skates, swimming is by undulations of their large elongated and highly flexible pectorals. The stingray swims forward by oscillating the fin rays slightly out of phase with each other, thereby producing a traveling wave along the fin, from front to back, to generate thrust while keeping its laterally compressed body mostly rigid. It can move backward with similar agility by reversing the direction of waveform propagation on its propulsor fin.

We captured the movement of a real bluespotted ray in order to observe the swimming mode of the fish and provide some useful references for biomimetic mechanism design. The bluespotted ray was free to swim in a big tank in NTU. Video recordings of rays swimming in the tank allowed roughly three-dimensional analysis of fin kinematics. Figure 4 to 8 shows some snapshots of swimming modes from cruising, through turning, to take-off and landing. As shown in the figures, the bluespotted ray is able to steer the movement by flapping up and down lateral fins with different amplitudes and frequencies.

**Cruising:** *Taeniura lymma* swims by passing waves along the pectoral fins from anterior to posterior (Fig. 4) while keeping its body stable. During steady forward swimming, both pectoral fins passed waves

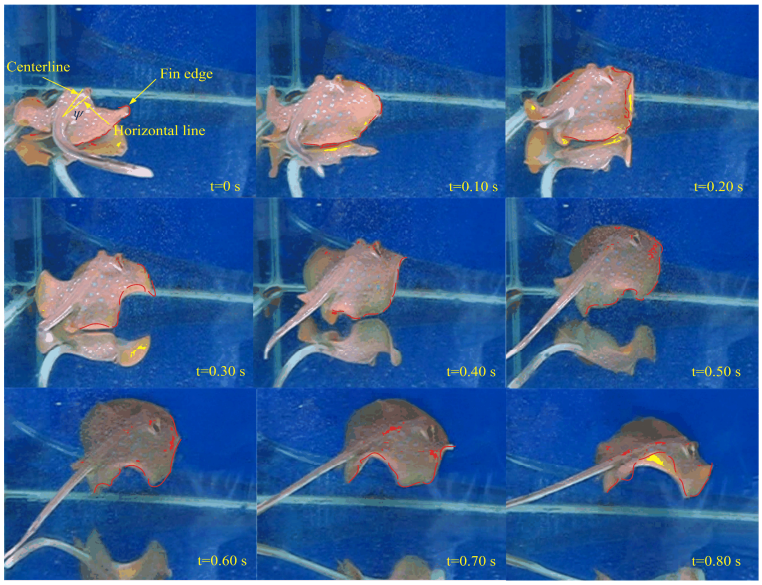


Fig. 6: Take-off of *Taeniura lymma*

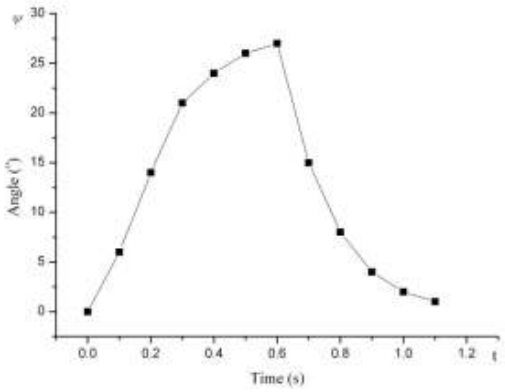


Fig. 7: Change of angle between centerline and horizontal line during take-off

down the fins simultaneously. We observed that: swimming velocity of *Taeniura lymma* is noticeably increased by increasing fin-beat frequency, there is an apparent trade-off between frequency and amplitude to achieve a given swimming speed, viz. a high fin-beat frequency is associated with a low fin amplitude, whereas a low fin-beat frequency is associated with a high fin amplitude, which are in agreement with Rosenberger's findings.

**Turning:** *Taeniura lymma* relies on the coordinated motion of slender tail and widely expanded pectoral fins to achieve its handling through turning. Figure 5 shows some snapshots of an anticlockwise 90$^{o}$ turning process. At the beginning, *Taeniura lymma* exhibits two remarkable characteristics, one is the asymmetric undulating of pectoral fins; the other one is the opposite swinging of its tail to the turning direction, thus generats rotating torque (due to fluid reaction force) relative to the center of gravity as marked in Fig. 5, while keeping its body straight. Later in the turning process, the tail inverses its swinging direction to produce auxiliary thrust for subsequent locomotion. Intriguingly, the center of gravity of *Taeniura lymma* has no obvious displacement during the whole turning process. The turning radius is almost zero, thus has extremely high maneuverability.

**Take-off and landing:** There are two types of ups-and-downs motion of fish, including dynamic and static. The dynamic ups and downs motion is controlled by adjusting the Angle Of Attack (AOA) of the body, providing vertical force. The static ups and downs motion is controlled by using of swim bladder or other organs to regulate their body density. *Taeniura lymma* belongs to cartilaginous fishes without swim bladder, so it must swim constantly to stay in a certain position. At the beginning of take-off, the anterior pectoral fin rays begin to oscillate. With a certain phase delay between fin rays, this volatility is then transfered to the posterior pectoral fin rays, and ultimately promote the formation of a stable wave (refer to Fig. 6 for more details).

Meanwhile, we measure the angle ψ, defined as the angle between body centerline and horizontal plane, during take-off process. As illustrated in Fig. 7, the angle increases from beginning to the maximum and tapers again almost to zero, this maximum angle is about 27°.

The landing process is characterized by: the amplitude and propogation velocity of undulatory wave decreases rapidly along the pectoral fin, the integrated effects of inertial force and fluid resistance result in the damped motion of fin. After a while, *Taeniura lymma* holds still on the bottom (Fig. 8).

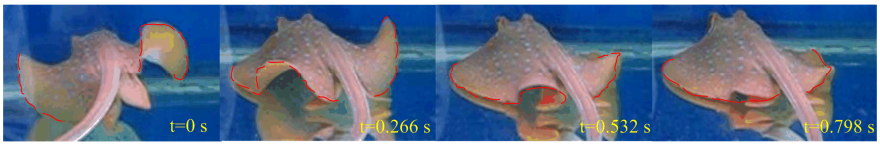


Fig. 8: Landing of *Taeniura lymma*

## MECHANICAL DESIGN

The above-mentioned morphology, kinematics and physiology observations will be used for morphological characteristics extraction and movement patterns description of bionic object. Moreover, it can also provide a reference for kinematics modeling and biomimetic mechanism development. For simplicity, we make several assumptions: firstly, the thickness of pectoral fins was neglected; secondly, the pectoral fin locomotion can be approximately described in sine wave form; finally, the fin ray baseline was reduced to a straight line, the spatial form of the swimming performance can be compensated by changing the fin ray length.

**Mechtronics:**

**Robotic bluespotted ray design:** The robotic *bluespotted ray* was designed with commercial three-dimensional CAD software (SolidWorks). All structural parts were precision cut from lightweight aluminum alloy sheets on a high-speed, CNC machine.

Figure 9 shows the mechanical structure of *bluespotted ray* like biorobotic underwater propulsor with a modular undulating fin consisting of eight equally spaced servomotors attached to a lightweight structure on both sides. As shown in Fig. 9, the prototype design of the developed robot, *bluespotted ray*, comprises of three individual modules: two pectoral fin modules, electronics housing module, center of gravity adjustment module. Tail is not considered for simplicity. There into, the fin ray element consists of axle sleeve, axle, steering-gear base, steering-gear support and steering-gear; the housing is used to install battery, control electronics and center of gravity adjustment module. All of them are installed on the baseboard. The prototype owns built-in energy source, it is a self sufficient prototype and gives an autonomy of 30 minutes of operation at moderate velocities. Meanwhile, two batteries provide the electrical energy required by electronics and control system components. The total batteries capacity is 3200 mAh. The mechanical design of the actuator system and the other sections provide robotic *bluespotted ray* the maximum interior capacity compared to the overall volume. This feature enables further modifications and makes the system suitable for additional accessory placements. The micro-controller (TI DSP, TMS320LF2407) based built-in control system controls the fin motions. Backed up with optical sensors which

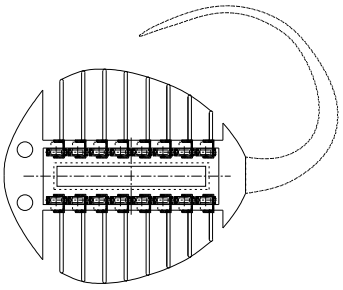

Fig. 9: Mechanical structure of robotic *bluespotted ray* (Zhang *et al*., 2012)

are used for environment exploration, this stand-alone system is the first step to the full autonomy of the prototype.

After the built of the prototype, we further conduct the experimental investigation to the influence of various kinematic parameters including frequency, amplitude and wavelength on the propulsion performance such as velocity, thrust and efficiency of the prototype.

## EXPERIMENTS

***Experiment set-up:*** The experimental setup consists of a high transparency tempered glass water tank (with working area dimension of 4.5 m×2 m×1.8 m), a high-speed camera system, a precision linear rail, transducers, a base and an indication of grid and reference grid coordinates (1×1 cm) (Zhang *et al*., 2012). The high-speed camera system (Model SpeedCAM) , which was lighted by two 1 kW tungsten lamps with the camera hanging over the tank, recorded images at a shutter speed of 1/250 s with maximum resolution ratio of 512×512 pixels. Video recordings were played back for digitization. Data were taken when the biorobot fin was swimming in the middle of the tank to minimize wall effects. A custom-designed digitizing program was used for measuring the x and y coordinates of marker on the fin and synchronously recording the time. Coordinate data were saved for further treatment.

## RESULTS AND DISCUSSIONS

**Effect of frequency:** Figure 10a to c show the effect of frequency (f) on the average propulsion velocity, the average output propulsion force and the average propulsion efficiency with A = 100 mm, = 387 mm. From the experiments, one

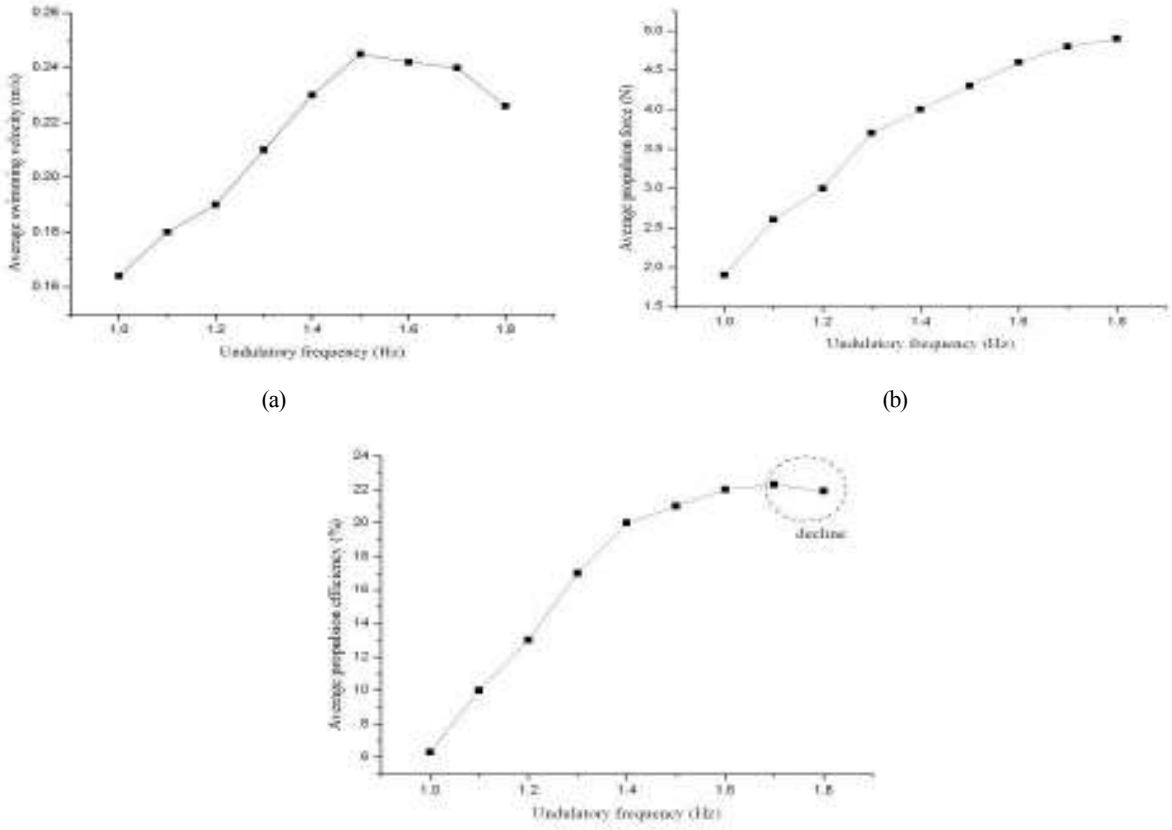


Fig. 10: Effect of frequency (f) on the average propulsion velocity, the average output propulsion force and the average propulsion efficiency with A = 100 mm, λ = 387 mm

would have expected to see an increasing trend up to a peak point at a frequency of around 1.5 Hz - 1.55 Hz at current condition, then followed by a decreasing trend. It was noted that the averaged output propulsion force increased as the frequency increased, but the slopes of the trend started to slow down. Moreover, the average propulsion efficiency is also increased as the frequency increased. When the frequency reached around 1.7 Hz, the efficiency began to decline. Hence, from the frequency point of view, it can be concluded that to obtain optimal propulsion performance, the undulatory frequency should be in a certain range. However, this range is changeable with different robotic systems.

**Effect of amplitude:** Figure 11a to c show the effect of amplitude (A) on the average propulsion velocity, the average output propulsion force and the average propulsion efficiency with f = 1.4 Hz, λ = 387 mm.

By virtue of Fig. 11, one can observe how the amplitude affects the multiple propulsion characteristics. The average propulsion velocity is increased as the amplitude increased. When the amplitude reached around 160 mm (22.5% of the total length of the biorobotic fin), the velocity began to decline (Fig. 11a). The propulsion efficiency also has the same change regularity as the propulsion velocity (Fig. 11c), which may be caused by the dramatic increase of vibration. As for Fig. 11b, it was noted that the output propulsion force increased as the amplitude increased. Although the peak of the curves is not appeared, the peak can be expected to be around 200 to 220 (28.2% to 31%) by looking at the trend of the curves.

**Effect of wavelength:** As can be seen from Fig. 12, the averaged propulsion velocity and force obviously increase with the increase of undulatory wavelength. However, on reaching the peak at a wavelength of around 710 mm (1 TL, TL: total length), the output propulsion force decreased with a further increase in wavelength. One of the probable reasons might be that the increase of wavelength will definitely flatten the curve shape of the fin, thus decrease the amount of the surrounded fluid, therefore propulsion force is then decreased. What's more, it was shown that the average propulsion efficiency increased as the wavelength increased. The efficiency peaked at a wavelength of around 1000 mm (1.25 TL). The average propulsion efficiency decreased with a further increase in

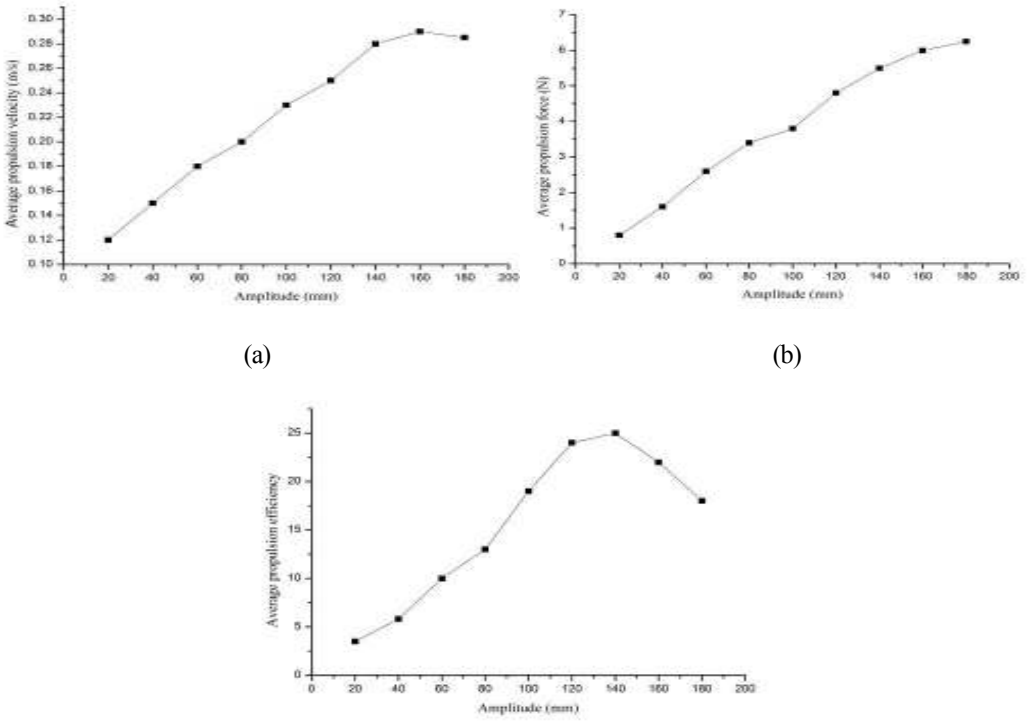


(a) (b)

(c)

Fig. 11: Effect of amplitude (A) on the average propulsion velocity, the average output propulsion force and the average propulsion efficiency with f = 1.4 Hz, λ = 387 mm

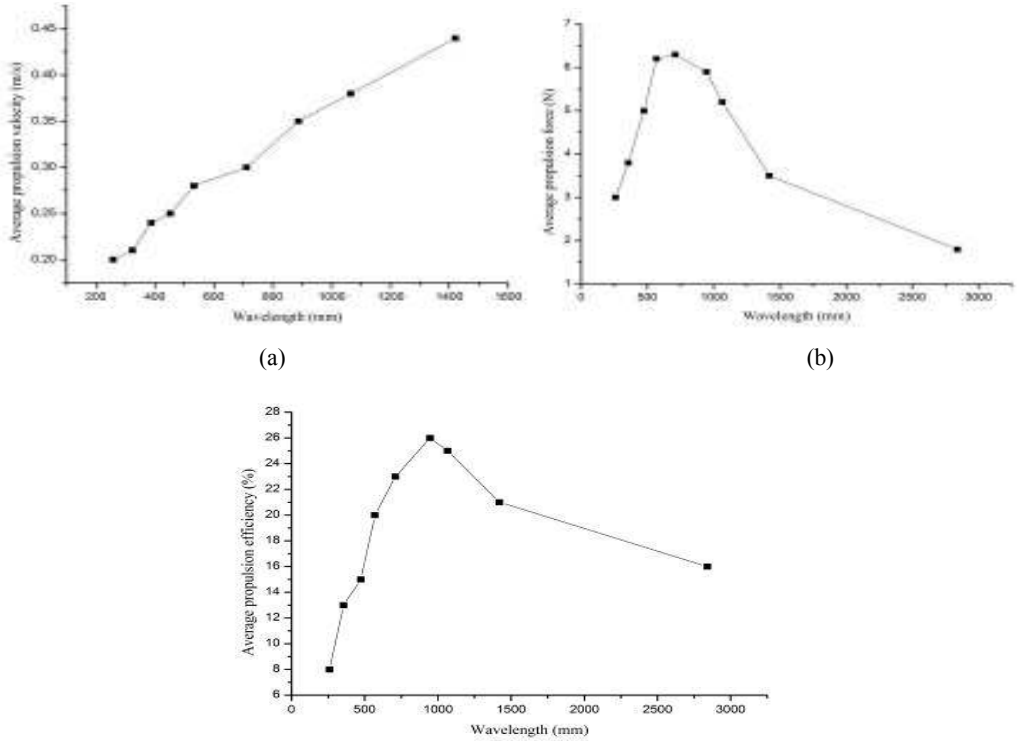


(a) (b)

(c)

Fig. 12: Effect of wavelength (λ) on the average propulsion velocity, the average output propulsion force and the average propulsion efficiency with f = 1.4 Hz, A = 100 mm

frequency. It was thought to have been caused by the reduced propulsion force which had been illustrated above.

## ACKNOWLEDGMENT

The authors would also like to thank Professor Jie Yang of University of Science and Technology of China for his support on the works over these years. This work was supported in part by the Scientific and Research Funds of Department of Education of Zhejiang Province through grant #Y201122502. The funds (2012ZD04) supported by TZVTC (Taizhou Vocational and Technical College) is also acknowledged.

## REFERENCES

Blake, R.W., 1979. The mechanics of labriform locomotion. I. Labriform locomotion in the angelfish (Pterophyllum eimekei): An analysis of the power stroke. J. Exp. Biol., 82: 255-271.

Blake, R.W., 1983. Swimming in the electric eels and knife fishes. Can. J. Zool., 61(6): 1432-1441.

Breder, C.M., 1926. The locomotion of fishes. Zoologica, 4: 159-297.

Calvert, R.A., 1983. Comparative anatomy and functional morphology of the pectoral fin of stingrays. MA Thesis, Duke University, Durham, NC, USA.

Chong, C.W., Y. Zhong and C.L. Zhou, 2009. Can the swimming thrust of BCF biomimetics fish be enhanced? Proceeding of the IEEE International Conference on Robotics and Biomimetics, Bangkok, Thailand, pp: 437-442.

Compagno, L.J.V., 2005. Taeniura Lymma. In: IUCN 2005. IUCN Red List of Threatened Species.

Epstein, M., J.E. Colgate and M.A. MacIver, 2006. Generating thrust with a biologically-inspired robotic ribbon fin. Proceedings of the 2006 IEEE/RSJ International Conference on Intelligent Robots and Systems, October 9-15, pp: 2412-2417.

Kato, N., 2000. Control performance in the horizontal plane of a fish robot with mechanical pectoral fins. IEEE J. Ocean Eng., 25(1): 121-129.

Leonard, N.E., 1995. Control synthesis and adaptation for an under actuated autonomous underwater vehicle. IEEE J. Ocean Eng., 20(3): 211-220.

Lighthill, J. and R. Blake, 1990. Biofluid dynamics of balistiform and gymnotiform locomotion 1. Biological background and analysis by elongated-body theory. J. Fluid Mech., 212(1): 183-207.

Lionel, L., 2006. Underwater Robots: Part I. In: Aleksandar, L. (Ed.), Current Systems and Problem Pose Mobile Robotics: Towards New Applications. Pro Literatur Verlag/ARS, Germany/Austria, pp: 335-360.

Low, K.H. and A. Willy, 2006. Biomimetic motion planning of an undulating robotic fish fin. J. Vib. Control., 12(12): 1337-1359.

MacIver, M.A., E. Fontaine and J.W. Burdick, 2004. Designing future underwater vehicles: Principles and mechanisms of the weakly electric fish. IEEE J. Ocean Eng., 29(3): 651-659.

Rosenberger, J.L., 2001. Pectoral fin locomotion in batoid fishes: Undulation versus oscillation. J. Exp. Biol., 204(2): 379-394.

Rosenberger, J.L. and M.W. Westneat, 1999. Functional morphology of undulatory pectoral fin locomotion in the stingray Taeniura lymma (chondrichthyes: Dasyatidae). J. Exp. Biol., 202(24): 3523-3539.

Saimek, S. and P.Y. Li, 2004. Motion planning and control of a swimming machine. Int. J. Robot. Res., 23(1): 27-53.

Standen, E.M., 2008. Pelvic fin locomotor function in fishes: Three-dimensional kinematics in rainbow trout (Oncorhynchus mykiss). J. Exp. Biol., 211(18): 2931-2942.

Videler, J.J., 1993. Fish Swimming. Chapman and Hall, London.

Vogel, S., 1994. Life in Moving Fluids. The Physical Biology of Flow. 2nd Edn., Princeton University Press, Princeton, NJ.

Walker, J.A. and M.W. Westneat, 2002. Performance limits of labriform propulsion and correlates with fin shape and motion. J. Exp. Biol., 205(2): 177-187.

Webb, P.W., 1973. Kinematics of pectoral fin propulsion in cymatogaster aggregata. J. Exp. Biol., 59: 697-710.

Webb, P.W., 1994. The Biology of Fish Swimming. In: Maddock, L., Q. Bone and J.M.V. Rayner (Ed.), Mechanics and Physiology of Animal Swimming. Cambridge University Press, Cambridge, UK, pp: 45-62.

Wernli, R.L., 1999. AUVs: The Maturity of the Technology MTS/IEEE OCEANS'99. Seattle, WA, pp: 189-195.

Zhang, Y.H., S.W. Zhang and J. Yang, 2007. Experimental research on crucian morphology. Reserv. Fish., 27(6): 79-81.

Zhang, Y.H., J.H. He and K.H. Low, 2012. Fin modeling and parametric study of an underwater propulsor inspired by Bluespotted ray. J. Bio. Eng., 9(2): 166-176.